ACS APPLIED MATERIALS & INTERFACES

Research Article

www.acsami.org

Monodisperse SnO_2-Coated Gold Nanoparticles Are Markedly More Stable than Analogous SiO_2-Coated Gold Nanoparticles

Sang Ho Lee, Irene Rusakova, David M. Hoffman, Allan J. Jacobson,* and T. Randall Lee*

Department of Chemistry and the Texas Center for Superconductivity, University of Houston, Houston, Texas 77204-5003, United States

Supporting Information

ABSTRACT: This manuscript describes the synthesis of uniform monodisperse SnO_2-coated gold nanoparticles and examines their colloidal stability as function of pH, with direct comparison to better known and widely used SiO_2-coated gold nanoparticles. Aqueous acidic and basic colloidal SnO_2-coated and SiO_2-coated Au nanoparticle solutions were prepared, and their stability was monitored visually and by UV−vis spectroscopy. Notably, the SnO_2-coated Au nanoparticle solutions were stable up to pH 12.5. However, at pH 13 and 14, the SnO_2-coated Au nanoparticles underwent aggregation, which could be fully reversed upon neutralization of the solutions. In contrast, the SiO_2-coated Au nanoparticle solutions were unstable at pH >10.5, irreversibly producing a precipitate composed of bare Au nanoparticle aggregates having little or no silica coating. Under acidic conditions, sedimentation was observed from both the colloidal SnO_2-coated and SiO_2-coated Au nanoparticle solutions, but the colloidal solutions could be reconstituted upon neutralization of the acidic solutions. The sedimentation at low pH coincided with the reported isoelectric pH values of SiO_2 and SnO_2, respectively. From an applications perspective, we are seeking to develop SnO_2-coated metal nanoparticles as stable alternatives to the more widely employed SiO_2-coated nanoparticles, with a particular emphasis on their use in sensor devices and solar cells.

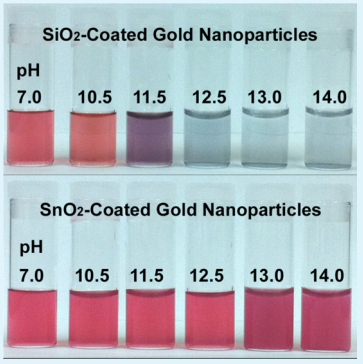

KEYWORDS: *SiO_2-coated nanoparticles, SnO_2-coated nanoparticles, colloidal stability, pH*

INTRODUCTION

Metal nanoparticles coated with metal oxides and/or semiconductors have become increasingly important in the past decade because of their potential applications in catalysis,[1] optical coatings,[2] sensing,[3,4] solar cells,[5] and nanomedicine.[6] The shell/core architecture affords enhanced luminescence for semiconductor nanoparticles, versatile bioconjugation, chemical and colloidal stability, and facile adjustment of the composition of the metal cores. A variety of metal oxides, including SiO_2,[1,6−8] TiO_2,[5,9−11] ZnO,[12−14] MnO_2,[15] Al_2O_3,[16] and SnO_2[2−4,17−19] have been used as the shell materials because they offer a range of refractive indexes and electrical conductivities. Among these shell/core nanoparticles, silica-coated metal nanoparticles are one of the most widely known because they are relatively easy to prepare, and they offer rich surface functionalization, high biocompatibility, controllable porosity, and good transparency. In particular, silica coatings have been widely used to prevent particle aggregation/sedimentation.

A number of methods have been used to synthesize silica-coated nanoparticles since the pioneering work by Mulvaney and co-workers in 1996.[7,20] In contrast, SnO_2-coated metal nanoparticles represent a related but markedly less studied class of shell/core nanoparticles; a search of the literature reveals only six prior reports of these species.[2−4,17−19] Tin(IV) oxide (SnO_2), as with silica (SiO_2), is also a suitable material for optical coatings because of transparency in the visible range. Furthermore, tin(IV) oxide is electroconductive and has consequently been used in the fabrication of transparent electrodes and infrared reflectors.[21]

We are interested in finding durable coatings for shell/core nanoparticles that can tolerate the potentially harsh environments encountered in certain sensing devices[4] and in many solar energy conversion applications, including photovoltaic devices and solar-to-hydrogen fuel cells.[22−25] A material commonly used in conventional solar conversion applications is tin(IV) oxide (SnO_2), which can be doped to form a transparent conductor.[26] Little is known about SnO_2-coated nanoparticles, however, and no studies of their stability or of the stability of their colloidal solutions under acidic or basic conditions have been published.[2−4,17,18] In this manuscript, we describe the synthesis of uniform monodisperse SnO_2-coated Au nanoparticles and examine their colloidal stability compared to SiO_2-coated Au nanoparticles over a wide pH range. We compared SnO_2-coated Au nanoparticles with SiO_2-coated Au nanoparticles specifically because of the widespread use of silica as a coating in core−shell nanoparticles.[1,6−8]

Received: November 18, 2012
Accepted: March 8, 2013

dx.doi.org/10.1021/am302740z | ACS Appl. Mater. Interfaces XXXX, XXX, XXX−XXX

EXPERIMENTAL SECTION

General Considerations. Commercial samples of chloroauric acid (Strem, 99.9% trace metals basis), 3-aminopropyltrimethoxysilane (Aldrich, 97%), sodium citrate (Aldrich, 99%), sodium silicate solution (Aldrich, reagent grade; ~10.6% Na_2O, ~26.5% SiO_2), and $Na_2SnO_3{\cdot}3H_2O$ (Aldrich, 95%) were used as received. All manipulations were performed in air. Deionized water was used in the synthetic preparations and stability studies. The syntheses of citrate-stabilized, SiO_2-coated, and SnO_2-coated Au nanoparticles were based on published procedures.[1−4,6−8,17,18]

Synthesis of Citrate-Stabilized Au Nanoparticles. In a beaker, 0.50 mL of chloroauric acid (1.9 g, 5.7 mmol) was diluted with water (150 mL), and the resulting solution was heated to boiling with stirring. An aliquot of a sodium citrate solution (10 mL, 1.0 wt %) was added quickly to the hot chloroauric acid solution with stirring. The color of the solution changed from light yellow to dark red within an hour. This red solution, presumed to contain citrate-stabilized gold nanoparticles, was allowed to cool to room temperature. The as-prepared solution was used subsequently in the syntheses of SnO_2- and SiO_2-coated Au nanoparticles as described below.

Synthesis of SnO_2-Coated Au Nanoparticles. A 5.0 mL aliquot of an aqueous solution of $Na_2SnO_3{\cdot}3H_2O$ (40 mM, 1.1 g, 0.20 mmol) was added rapidly with stirring to a 500 mL round-bottomed flask containing 150 mL of heated (80 °C) aqueous citrate-stabilized gold nanoparticle solution (prepared as described above). A pink solution was obtained immediately. The solution was cooled to room temperature and centrifuged (6000 rpm/30 min). The supernatant liquid was removed with a pipet and discarded. Water was added to the resultant sticky solid, giving a pink colloidal solution.

Synthesis of SiO_2-Coated Au Nanoparticles. A 1.0 mL aliquot of a freshly prepared aqueous solution of 3-aminopropyltrimethoxysilane (1.0 mM, 1.8×10^{-4} g, 1.0×10^{-3} mmol) was added with vigorous stirring to 100 mL of the aqueous citrate-stabilized gold nanoparticle solution in a 500 mL round-bottomed flask. After the addition was complete, the mixture was stirred at room temperature for 30 min. The mixture was then heated to 80 °C with vigorous stirring, and a 1.0 mL aliquot of an aqueous solution of sodium silicate (1 wt %) was added rapidly. A pink colloidal solution was obtained immediately. The solution was cooled to room temperature and centrifuged (6000 rpm/30 min). The supernatant liquid was removed with a pipet and discarded. Water was added to the resultant sticky solid, giving a pink colloidal solution.

Nanoparticle Characterization. The size and morphology of uncoated and coated Au nanoparticles were determined using a JEOL JEM-2000 FX transmission electron microscope (TEM) operating at a bias voltage of 200 kV. The samples for TEM analyses were prepared by placing a drop of the colloidal solution from a pipet onto a carbon-coated copper TEM grid and then drying in air. This process was repeated (10 times or more) to obtain a quantity of sample suitable for analysis.

UV−vis spectra were obtained in the range 400−1000 nm using a Cary 50 Scan UV−vis spectrometer. The samples for analyses were prepared by placing the as-prepared aqueous solutions in quartz cuvettes.

X-ray photoelectron spectroscopy (XPS) data were collected on a Physical Electronics Model 5700 instrument. Photoemission spectra were produced using a monochromatic Al Kα X-ray source (1486.6 eV) operated at 350 W. The XPS samples for analysis were prepared by placing a drop of the colloidal solution from a pipet onto a silicon wafer (NESTEC, ⟨100⟩) and then drying in air. This process was repeated (10 times or more) to obtain a quantity of a sample suitable for analysis. XPS scans were conducted at high resolution with pass energy 23.5 eV, a photoelectron takeoff angle of 45°, and an analyzer spot diameter of 2 nm. The Sn 3d, O 1s, and C 1s binding energies were referenced to the Au $4f_{7/2}$ peak (84 eV).

Stability Studies. The pH of colloidal solutions was adjusted using 0.1 M solutions of HCl, NaOH, and CsOH, as appropriate, and was measured by using pH test paper (EMD Chemicals ColorpHast). The solutions were monitored visually for the appearance of a precipitate and/or a color change, and a UV−vis spectrum was collected for each solution to compare with the spectrum of the parent solution. In selected cases, precipitates were collected with a pipet and placed on a silicon wafer for analysis by XPS as described above.

RESULTS AND DISCUSSION

Citrate-stabilized, SnO_2-coated[2−4,17−19] and SiO_2-coated[1,6−8] gold nanoparticles were synthesized using procedures adapted from the indicated literature references. Scheme 1 illustrates the synthetic procedures used. First, gold nanoparticles were synthesized using a common sodium citrate reduction method.[27] The preparation of the SnO_2-coated Au nanoparticles involves the spontaneous encapsulation of the Au nanoparticles within the tin(IV) oxide shell upon the addition of sodium stannate trihydrate ($Na_2SnO_3{\cdot}3H_2O$) via a simple hydrothermal process. The preparation of the SiO_2-coated Au nanoparticles involves surface functionalization with with 3-aminopropyl trimethoxysilane (APTMS) in aqueous solution. In this process, the NH_2 groups bind to the surface of gold, and the $Si(OEt)_3$ groups are extended outward for hydrolysis and condensation with sodium silicate (Na_2SiO_3) to deposit a thin layer of silica.

Scheme 1. Synthesis of SiO_2-Coated Au Nanoparticles and SiO_2-Coated Au Nanoparticles

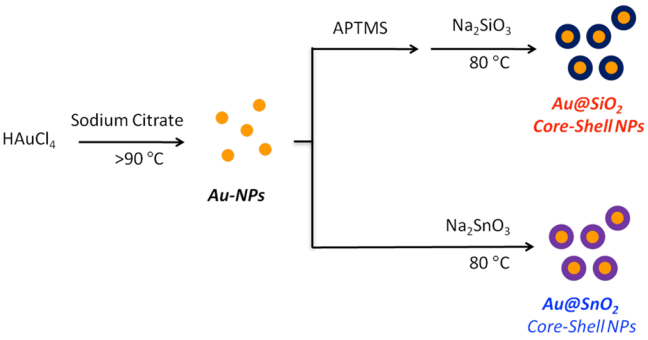

According to Mulvaney,[17] to coat SnO_2 onto the gold particles, the pH of the Au colloid solution was first adjusted to 10.5 with sodium hydroxide. Sodium stannate was then added to the Au particles, and the basic solution was stirred and heated to 60 °C for 1 h. In the work reported here, we followed the original synthetic method, but employed modifications to obtain more uniform and monodisperse shell/core particles. In particular, we made the following three changes, which are detailed in the Experimental Section: (1) we omitted the adjustment of pH with sodium hydroxide, (2) we used a different amount of sodium stannate solution, and (3) we heated the solution to 80 °C rather than 60 °C.

Figure 1 shows TEM images of the nanoparticles. For all samples, the Au nanoparticle diameter is about 15 nm. The thicknesses of the SiO_2 and SnO_2 coatings are approximately 7 and 10 nm, respectively, giving rise to composite particle diameters of ~30 and ~35 nm, respectively. In the sample of the nanoparticles collected from the SnO_2-coated Au nanoparticle solutions, gold-free SnO_2 nanoparticles were also observed, representing approximately 10% of the samples. The TEM images show that all of the shell/core nanoparticles have excellent uniformity; notably, the SnO_2-coated Au nanoparticles show greater uniformity than those reported previously.[2−4,17,18] Also, the thicknesses of the SnO_2 shells

dx.doi.org/10.1021/am302740z | ACS Appl. Mater. Interfaces XXXX, XXX, XXX−XXX

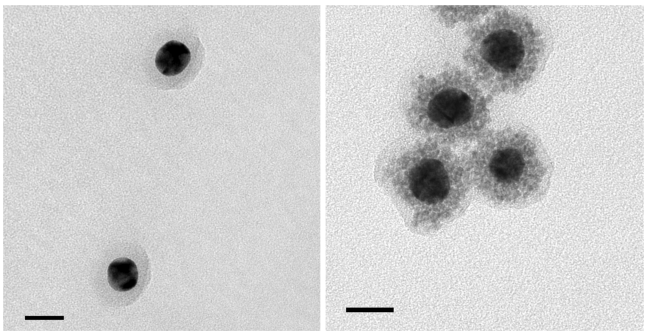

Figure 1. TEM images of (left) SiO_2-coated gold nanoparticles and (right) SnO_2-coated gold nanoparticles. The scale bars are 20 nm.

could be readily varied from 5 to 20 nm (see Figures S1−S3 in the Supporting Information).

Figure 2 shows the extinction spectra of the colloidal uncoated and coated Au nanoparticle solutions. The surface plasmon resonance (SPR) observed for the citrate-stabilized, SiO_2-coated, and SnO_2-coated Au nanoparticle solutions had maxima at 522, 529, and 533 nm, respectively, consistent with previously reported values.[17,28] The red shifts of the SPR bands for the coated particles are due to the high refractive indexes of the SiO_2 (1.46)[29] and SnO_2 (2.2)[30] coatings. Notably, the SPR band of the SnO_2-coated particles was observed to undergo a red shift with increasing thickness of the SnO_2 layer (see Figure S4 in the Supporting Information).

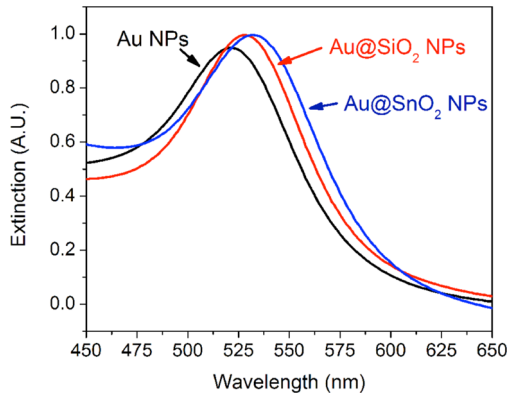

Figure 2. Extinction spectra of citrate-stabilized Au nanoparticles (Au NPs), SiO_2-coated Au nanoparticles (Au@SiO_2 NPs), and SnO_2-coated Au nanoparticles (Au@SnO_2 NPs).

To determine the stability of the coated nanoparticles and their colloidal solutions under acidic and basic conditions, colloidal nanoparticle solutions with various pH values were prepared and monitored over time by visual inspection and collection of extinction spectra. Figure 3 shows photographs of colloidal SiO_2-coated and SnO_2-coated Au nanoparticle solutions under neutral and basic conditions. The color changes observed for the SiO_2-coated Au nanoparticle solutions (Figure 3a), which occurred within a few minutes of adjusting the pH, indicate that the solutions were unstable under basic conditions.

Extinction spectra (Figure 4a) were consistent with the visual observations. The blue shift of the SPR band maxima to 522 nm for the solution at pH 10.5 (Figure 4a) is consistent with the formation of a bare Au nanoparticles, and the spectra for the solutions with pH >10.5 are consistent with the aggregation

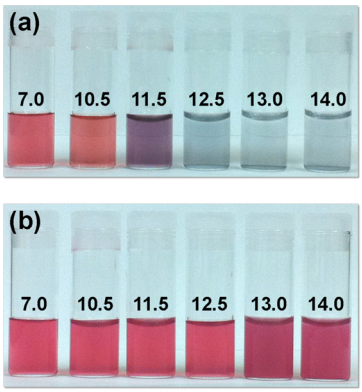

Figure 3. Photographs of colloidal (a) SiO_2-coated Au nanoparticle and (b) SnO_2-coated Au nanoparticle solutions at various pH values. The photographs were taken approximately 1 h after the solution pH values were adjusted using 0.1 M NaOH. The loss of dispersion for the SiO_2-coated Au nanoparticles at high pH, however, occurred immediately upon adjustment of the pH.

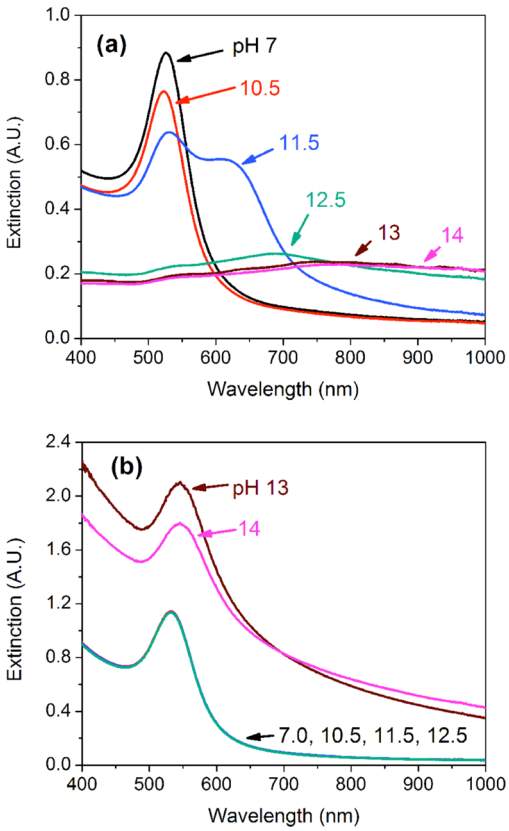

Figure 4. Extinction spectra of colloidal (a) SiO_2-coated Au nanoparticles and (b) SnO_2-coated Au nanoparticle solutions at various pH values. The spectra were recorded approximately 1 h after the solution pH values were adjusted using 0.1 M NaOH.

and sedimentation of bare Au nanoparticles.[31,32] The behavior observed for the SiO_2-coated nanoparticle solutions at high pH can be attributed to the solubility of SiO_2 in basic solution: at high pH, the SiO_2 coating dissolves,[33] leaving the mostly bare Au nanoparticles to aggregate.[31,32] This interpretation is supported by TEM images and XPS spectra of the aggregated particles (please see Figure S5 and Table S1 in the Supporting Information).

dx.doi.org/10.1021/am302740z | ACS Appl. Mater. Interfaces XXXX, XXX, XXX−XXX

In contrast to the behavior exhibited by the SiO_2-coated Au nanoparticle solutions at high pH, the SnO_2-coated Au nanoparticle solutions appeared to be stable at high pH after 1 h by visual inspection (Figure 3b). This apparent stability up to pH 12 was observed for at least several weeks (data not shown). We note, however, that at pH 13 and 14 only, the SnO_2-coated nanoparticle solutions displayed evidence of sedimentation after 24 h. The apparent stability of the SnO_2-coated Au nanoparticle solutions under basic conditions is corroborated by extinction spectra (Figure 4b). The SPR band maxima of the SnO_2-coated Au nanoparticles were centered at 533 nm for solution pH 7−12, consistent with a stable colloidal solution. At pH 13 and 14, however, the SPR maxima were red-shifted (545 nm), and the magnitude of extinction increased because of the increase in the size of the clusters upon nanoparticle aggregation and the consequent increase in scattering.[34]

We propose that the nanoparticle aggregation at pH 13−14 is induced by the presence of a high concentration sodium cations. Sodium cations in the solution can plausibly destabilize colloidal suspensions due to strong interactions between the sodium cations and the negatively charged SnO_2 surface.[35] Scheme 2 shows how bridging interactions give rise to clustering of the particles.

Scheme 2. Illustration of the Bridging Interactions between Sodium Ions and the Negatively Charged Surface of SnO_2−Coated Gold Nanoparticles at High pH

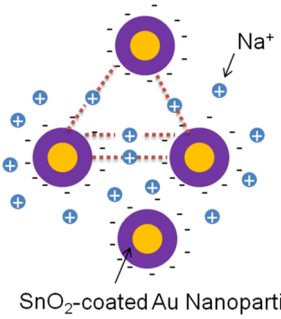

Interestingly, the effect was fully reversible: when the pH 13 and 14 solutions were adjusted to pH 12.5 with 0.1 M HCl and the extinction spectra remeasured, the SPR maxima shifted to 533 nm, consistent with reconstitution of the stable colloidal SnO_2-coated Au nanoparticle solution. These results suggest that at pH 13 and 14 the SnO_2 coatings remain intact despite the aggregation; this interpretation is supported by TEM images and XPS spectra of the particles exposed to highly basic solution (please see the data below and in the Supporting Information). A possible rationalization for the reversible aggregation is that at high pH, highly charged (deprotonated) SnO_2-coated Au nanoparticles are formed, and these charged species interact with Na^+ to form clusters.[35] In contrast, the nanoparticles at lower pH are not as highly charged and consequently do not extensively form clusters with Na^+.[35]

To test the notion of whether the aggregation of SnO_2-coated Au nanoparticles at high pH depends specifically on the intermediacy of Na^+, the experiments for SnO_2-coated Au nanoparticle solutions were repeated using CsOH to adjust the pH. As shown in the spectra presented in Figure 5, the SPR peak maxima for the pH 13 and 14 solutions are not red-shifted, in contrast to when Na^+ was present. We attribute this

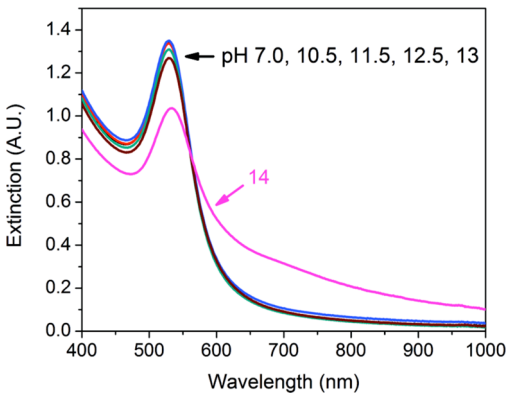

Figure 5. Extinction spectra of colloidal SnO_2-coated Au nanoparticle solutions at various pH values. The spectra were recorded approximately 1 h after the pH values were adjusted with 0.1 M CsOH.

phenomenon to the lower charge density of Cs^+ compared to Na^+, which in turn leads to diminished cluster formation at high pH.

Support for our model can be found in a recent report by Grzybowski and co-workers that rationalizes how the electrostatic stabilization of nanoparticles can fail as the surface charge of the particles increases.[35] Specifically, the bridging interactions between like-charged nanoparticles and cations (NP-M^+-NP) alter the electrodynamic coupling between particle cores, which can lead to aggregation and a concomitant change in the color of the solution. The order of critical salt concentrations required to precipitate particles having the same charge is $Cs^+ \gg K^+ > Li^+ > Na^+ > Rb^+$. Importantly, this trend fails to correlate with the size of hydrated cations M^+, nor is it predicted by the Hofmeister series. Therefore, in our system, Na^+ ions in the presence of SnO_2-coated Au nanoparticles give rise to more bridging interactions than do Cs^+ ions, which leads to enhanced aggregation/sedimentation only in the former system.

The stabilities of the colloidal nanoparticle solutions were also compared under acidic conditions. In Figure 6, photographs are presented showing the SiO_2-coated and SnO_2-coated Au nanoparticle solutions at low pH. Over the pH range 2−7, the SiO_2-coated Au nanoparticles displayed excellent dispersion (Figure 6a), and the SPR peak maxima at 529 nm in the

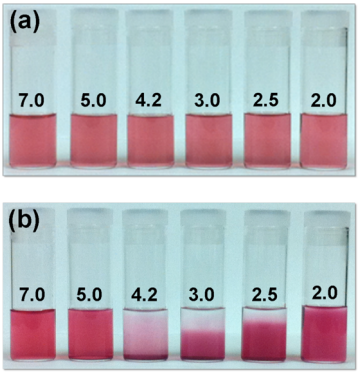

Figure 6. Photographs of colloidal (a) SiO_2-coated Au nanoparticles and (b) SnO_2-coated Au nanoparticle solutions at various pH values. The photographs were taken approximately one hour after the pH values were adjusted with 0.1 M HCl.

dx.doi.org/10.1021/am302740z | ACS Appl. Mater. Interfaces XXXX, XXX, XXX−XXX

corresponding extinction spectra were invariant (Figure 7a). In contrast, at pH 2−4 the nanoparticles precipitated from the

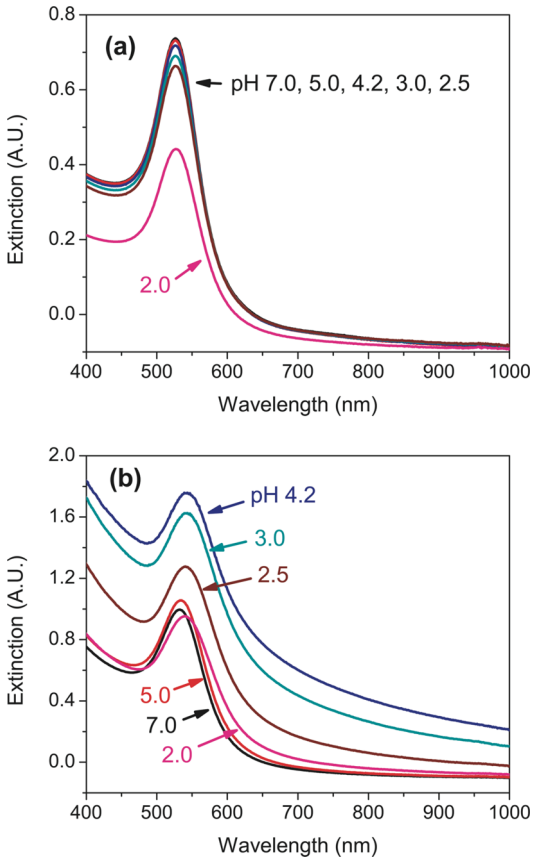

Figure 7. Extinction spectra of colloidal (a) SiO_2-coated gold nanoparticle and (b) SnO_2-coated Au nanoparticle solutions at various pH values. The spectra were recorded approximately one hour after the pH values were adjusted using 0.1 M HCl.

SnO_2-coated Au nanoparticle solutions (Figure 6a), with the precipitation rate increasing with increasing pH. The aggregation was reflected in the extinction spectra, which showed a red shift for the SPR maxima to 542−545 nm for the pH 2.0, 2.5, 3.0, and 4.2 solutions from the maxima at 533 nm for pH 7. The contrasting behavior between the SiO_2-coated vs SnO_2-coated nanoparticle solutions at pH 2−4 corresponds with the different isoelectric points of SiO_2 and SnO_2: the point of zero charge for SiO_2 and SnO_2 sols and gels are ∼2 and ∼4.0−4.5, respectively.[36,37] At the pH corresponding to the zero-point charge, there is no net surface charge on the particles; as such, interparticle interactions are governed by attractive van der Waals forces that readily give rise to aggregation and sedimentation. Because the zero-point charge of SnO_2 occurs at pH 4.0−4.5, it is reasonable that Figure 6b shows the greatest sedimentation for SnO_2-coated Au nanoparticles when the pH is reduced to 4.2. As the pH is reduced further, the degree of sedimentation diminishes systematically as the surface of the particles becomes protonated, and the particles consequently become electrostatically stabilized in solution.

Correspondingly, the SiO_2-coated nanoparticles precipitated slowly (∼7 days) at pH 2, but there was no sedimentation from solutions with pH >2. Colloidal solutions of the SiO_2 and SnO_2-coated nanoparticles reformed upon neutralization of the solutions from which sedimentation had occurred. The reversibility suggests that the coatings remained intact (vide supra).

X-ray photoelectron spectroscopy (XPS) studies were performed to determine the species present in the SnO_2-coated Au nanoparticles that precipitated from solutions at pH 4.2 and 13. For comparison, XPS data were also collected for particles collected from a colloidal solution at pH 7. The spectra for the three samples shown in Figure 8 are similar, with

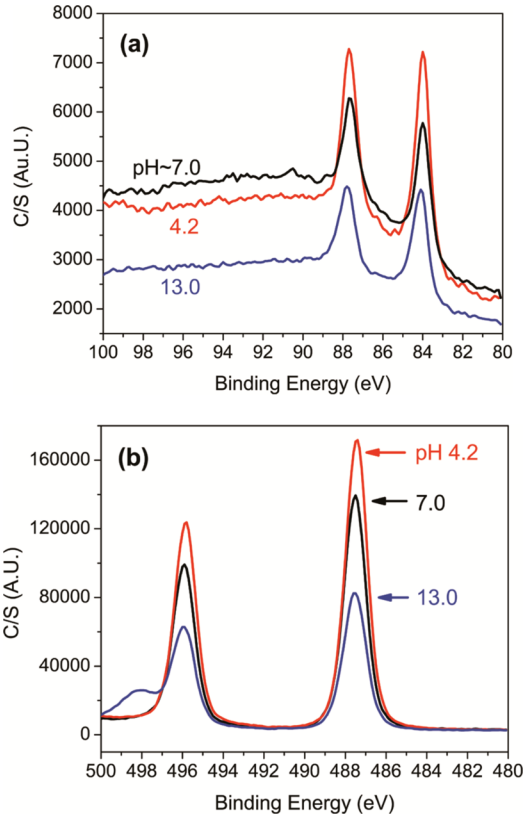

Figure 8. High-resolution XPS spectra of SnO_2-coated Au nanoparticles that precipitated from solution at pH 4.2 and 13; (a) Au_{4f} and (b) Sn_{3d}. Data were also collected from a colloidal solution at pH 7 for comparison. The peak at 498 eV at pH 13 can be assigned to a sodium Auger signal (Na_{KLL}).

each revealing peaks at 84.0 and 87.7 eV assigned to Au^0 $4f_{7/2}$ and $4f_{5/2}$, respectively,[38,39] and peaks at 487.4 and 495.8 eV assigned to Sn^{4+} $3d_{5/2}$ and $3d_{3/2}$, respectively.[40] These data are consistent with the presence of intact SnO_2-coated Au nanoparticles, suggesting that sedimentation of the particles is not accompanied by removal of the SnO_2 coating. This stability is corroborated by the observation of reversible colloid formation upon neutralization of the solutions from which sedimentation had occurred.

CONCLUSIONS

By modifying an existing synthetic method, we prepared uniform monodisperse SnO_2-coated Au nanoparticles and compared their stability to that of the better known and more widely used SiO_2-coated Au nanoparticles. Our studies found that the SnO_2-coated Au nanoparticles in aqueous solution are more stable under basic conditions (up to pH 14) than analogous SiO_2-coated Au nanoparticles. The instability of the SiO_2-coated Au nanoparticles at high pH is due to the

dx.doi.org/10.1021/am302740z | ACS Appl. Mater. Interfaces XXXX, XXX, XXX−XXX

dissolution of the SiO_2 coating. Although the SnO_2-coated nanoparticles were observed to precipitate at extremely high pH (i.e., pH 13 and 14 only), the precipitation was fully reversible upon neutralization, and the SnO_2 coating remained intact. We proposed that the latter sedimentation arises from bridging interactions between Na^+ ions and the negatively charged surface of the SnO_2-coated nanoparticles at high pH. Additionally, we observed sedimentation at low pH for both SiO_2- and SnO_2-coated Au nanoparticles, and the pH at which sedimentation was observed coincided approximately with the isoelectric pH values of the oxides. The sedimentation at low pH was also fully reversible upon neutralization of the solution. As a whole, the results demonstrate that SnO_2 is a durable coating for metal nanoparticles.

■ ASSOCIATED CONTENT

Supporting Information

TEM image and XPS spectra for the SiO_2-coated nanoparticles that aggregated at high pH, and analogous data for the unaggregated SnO_2-coated nanoparticles exposed to high pH; TEM images and extinction spectra of SnO_2-coated nanoparticles with varying shell thickness. This material is available free of charge via the Internet at http://pubs.acs.org.

■ AUTHOR INFORMATION

Corresponding Author

*E-mail: ajjacob@uh.edu (A.J.J.); trlee@uh.edu (T.R.L.).

Notes

The authors declare no competing financial interest.

■ ACKNOWLEDGMENTS

The Texas Center for Superconductivity and the Robert A. Welch Foundation (Grants E-1206, E-0024, and E-1320) supported this research. We thank Dr. James K. Meen for assistance with the SEM images, Bo Sang Kim for assistance with the images, and Dr. Boris Makarenko for assistance with the XPS measurements.

■ REFERENCES

(1) Joo, S. H.; Park, J. Y.; Tsung, C.-K.; Yamada, Y.; Yang, P.; Somorjai, G. A. *Nat. Mater.* **2009**, *8*, 126−131.
(2) Tripathy, S. K.; Jo, J.-N.; O, K.-J.; Han, S.-D.; Lee, I.-H.; Yu, Y.-T. *J. Mater. Sci.: Mater. Electron.* **2010**, *21*, 758−764.
(3) Yu, K.; Wu, Z.; Zhao, Q.; Li, B.; Xie, Y. *J. Phys. Chem. C* **2008**, *112*, 2244−2247.
(4) Yu, Y.-T.; Dutta, P. *Sens. Actuators, B* **2011**, *157*, 444−449.
(5) Standridge, S. D.; Schatz, G. C.; Hupp, J. T. *Langmuir* **2009**, *25*, 2596−2600.
(6) Liu, S.; Han, M. *Adv. Funct. Mater.* **2005**, *15*, 961−967.
(7) Liz-Marzan, L. M.; Giersig, M.; Mulvaney, P. *Langmuir* **1996**, *12*, 4329−4335.
(8) Ung, T.; Liz-Marzan, L. M.; Mulvaney, P. *J. Phys. Chem. B* **2001**, *105*, 3441−3452.
(9) Pastoriza-Santos, I.; Koktysh, D. S.; Mamedov, A. A.; Giersig, M.; Kotov, N. A.; Liz-Marzan, L. M. *Langmuir* **2000**, *16*, 2731−2735.
(10) Wu, X.-F.; Song, H.-Y.; Yoon, J.-M.; Yu, Y.-T.; Chen, Y.-F. *Langmuir* **2009**, *25*, 6438−6447.
(11) Li, J.; Zeng, H. C. *Angew. Chem., Int. Ed.* **2005**, *44*, 4342−4345.
(12) Haldar, K. K.; Patra, A. *Appl. Phys. Lett.* **2009**, *95*, 063103/1−063103/3.
(13) Haldar, K. K.; Sen, T.; Patra, A. *J. Phys. Chem. C* **2008**, *112*, 11650−11656.
(14) Sun, L.; Wei, G.; Song, Y.; Liu, Z.; Wang, L.; Li, Z. *Mater. Lett.* **2006**, *60*, 1291−1295.
(15) Lin, X.-D.; Uzayisenga, V.; Li, J.-F.; Fang, P.-P.; Wu, D.-Y.; Ren, B.; Tian, Z.-Q. *J. Raman Spectrosc.* **2011**, *43*, 40−45.
(16) Li, J. F.; Huang, Y. F.; Ding, Y.; Yang, Z. L.; Li, S. B.; Zhou, X. S.; Fan, F. R.; Zhang, W.; Zhou, Z. Y.; Wu, D. Y.; Ren, B.; Wang, Z. L.; Tian, Z. Q. *Nature* **2010**, *464*, 392−395.
(17) Oldfield, G.; Ung, T.; Mulvaney, P. *Adv. Mater.* **2000**, *12*, 1519−1522.
(18) Yu, Y.-T.; Dutta, P. *J. Solid State Chem.* **2011**, *184*, 312−316.
(19) Yanagimoto, T.; Yu, Y. T.; Kaneko, K. *Sens. Actuators, B* **2012**, *166−167*, 31−35.
(20) Liu, S.; Han, M.-Y. *Chem.—Asian J.* **2010**, *5*, 36−45.
(21) Ray, S.; Dutta, J.; Barua, A. K.; Deb, S. K. *Thin Solid Films* **1991**, *199*, 201−7.
(22) Brown, M. D.; Suteewong, T.; Kumar, R. S. S.; D'Innocenzo, V.; Petrozza, A.; Lee, M.; Wiesner, U.; Snaith, H. J. *Nano Lett.* **2011**, *11*, 438−445.
(23) Qu, D.; Liu, F.; Yu, J.; Xie, W.; Xu, Q.; Li, X.; Huang, Y. *Appl. Phys. Lett.* **2011**, *98*, 113119/1−113119/3.
(24) Hsu, R. S.; Higgins, D.; Chen, Z. *Nanotechnology* **2010**, *21*, 165705/1−165705/5.
(25) Luo, J.; Wang, L.; Mott, D.; Njoki, P. N.; Lin, Y.; He, T.; Xu, Z.; Wanjana, B. N.; Lim, I. I. S.; Zhong, C.-J. *Adv. Mater.* **2008**, *20*, 4624.
(26) Batzill, M.; Diebold, U. *Prog. Surf. Sci.* **2005**, *79*, 47−154.
(27) Enustun, B. V.; Turkevich, J. *J. Am. Chem. Soc.* **1963**, *85*, 3317−28.
(28) Correa-Duarte, M. A.; Sobal, N.; Liz-Marzan, L. M.; Giersig, M. *Adv. Mater.* **2004**, *16*, 2179−2184.
(29) Philipse, A. P.; Vrij, A. *J. Colloid Interface Sci.* **1989**, *128*, 121−36.
(30) Kim, T. W.; Lee, D. U.; Choo, D. C.; Yoon, Y. S. *Appl. Phys. Lett.* **2001**, *79*, 2187−2189.
(31) Aryal, S.; Bahadur, K. C. R.; Bhattarai, N.; Kim, C. K.; Kim, H. Y. *J. Colloid Interface Sci.* **2006**, *299*, 191−197.
(32) Shim, J.-Y.; Gupta, V. K. *J. Colloid Interface Sci.* **2007**, *316*, 977−983.
(33) Alexander, G. B.; Heston, W. M.; Iler, R. K. *J. Phys. Chem.* **1954**, *58*, 453−455.
(34) Kim, Y.; Johnson, R. C.; Hupp, J. T. *Nano Lett.* **2001**, *1*, 165−167.
(35) Wang, D.; Tejerina, B.; Lagzi, I.; Kowalczyk, B.; Grzybowski, B. A. *ACS Nano* **2011**, *5*, 530−536.
(36) Parks, G. A. *Chem. Rev.* **1965**, *65*, 177−198.
(37) Johansen, P. G.; Buchanan, A. S. *Aust. J. Chem.* **1957**, *10*, 398−403.
(38) Joseph, Y.; Besnard, I.; Rosenberger, M.; Guse, B.; Nothofer, H.-G.; Wessels, J. M.; Wild, U.; Knop-Gericke, A.; Su, D.; Schloegl, R.; Yasuda, A.; Vossmeyer, T. *J. Phys. Chem. B* **2003**, *107*, 7406−7413.
(39) Maye, M. M.; Luo, J.; Lin, Y.; Engelhard, M. H.; Hepel, M.; Zhong, C.-J. *Langmuir* **2003**, *19*, 125−131.
(40) Ansari, S. G.; Dar, M. A.; Kim, Y.-S.; Kim, G.-S.; Seo, H.-K.; Khang, G.; Shin, H.-S. *Appl. Surf. Sci.* **2007**, *253*, 4668−4672.